Research Article

MOLECULAR PAIN

Molecular Pain
Volume 14: 1–13

DOI: 10.1177/1744806918781733
journals.sagepub.com/home/mpx
SAGE

Dehydrocorydaline attenuates bone cancer pain by shifting microglial M1/M2 polarization toward the M2 phenotype

Wenwen Huo[1,*], Ying Zhang[1,*], Yue Liu[1], Yishan Lei[1], Rao Sun[1], Wei Zhang[1], Yulin Huang[1], Yanting Mao[1], Chenchen Wang[1], Zhengliang Ma[1], and Xiaoping Gu[1]

Abstract

Bone cancer pain remains a major challenge in patients with primary or metastatic bone cancer due to a lack of understanding the mechanisms. Previous studies have revealed the two distinct functional polarization states of microglia (classically activated M1 and alternatively activated M2) in the spinal cord in nerve injury–induced neuropathic pain. However, whether microglia in the spinal cord polarize to M1 and M2 phenotypes and contribute to the development of bone cancer pain remains unclear. In this study, we used a mouse model with bone cancer to characterize the M1/M2 polarization of microglia in the spinal cord during the development of bone cancer pain, and investigated the antinociceptive effects of dehydrocorydaline, an alkaloidal component isolated from *Rhizoma corydalis* on bone cancer pain. Our results show that microglia in the spinal cord presented increased M1 polarization and decreased M2 polarization, while overproduction of IL-1β and inhibited expression of IL-10 was detected during bone cancer pain development. Intraperitoneal administration of dehydrocorydaline (10 mg/kg) had significant antinociceptive effects on day 14 after osteosarcoma cell implantation, accompanied by suppressed M1 phenotype and upregulated M2 phenotype of microglia in the spinal cord, while alleviated inflammatory response was observed then. These results suggest that the imbalanced polarization of microglia toward the M1 phenotype in the spinal cord may contribute to the development of bone cancer pain, while dehydrocorydaline helps to attenuate bone cancer pain, with microglial polarization shifting toward the M2 phenotype in the spinal cord.

Keywords

Bone cancer pain, microglia, polarization, M1 phenotype, M2 phenotype, dehydrocorydaline

Date Received: 10 February 2018; revised: 13 April 2018; accepted: 11 May 2018

Introduction

Bone cancer pain (BCP) is one of the most common pain syndromes encountered in patients with primary or metastatic bone cancer of the breast, lung, and prostate, seriously compromising quality of life for many patients.[1,2] As detection and survival among patients with cancer have improved, cancer-induced pain has become an increasing challenge.[3] However, pharmacological managements are still unsatisfactory and far from all patients obtain sufficient pain relief currently. The mechanisms underlying this chronic pain remain to be investigated, and effective therapies are urgently needed to improve this situation.

Microglia are the primary immune effector cells in the spinal cord. They become activated and undergo morphological as well as functional transformations in response to any kind of spinal cord damage or injury.[4,5] Several studies have demonstrated that microglial

[1]Department of Anesthesiology, Affiliated Drum Tower Hospital of Medical Department of Nanjing University, Nanjing, China

*The first two authors contributed equally to this work.

Corresponding Authors:
Zhengliang Ma, Department of Anesthesiology, Affiliated Drum Tower Hospital of Medical Department of Nanjing University, 321 Zhongshan Road, Nanjing 210008, China.
Email: mazhengliang1964@nju.edu.cn
Xiaoping Gu, Department of Anesthesiology, Affiliated Drum Tower Hospital of Medical Department of Nanjing University, 321 Zhongshan Road, Nanjing 210008, China.
Email: xiaopinggu@nju.edu.cn

activation in the spinal cord plays an important role in the pathological changes, which contribute to the generation and maintenance of BCP.[6–8] The activated microglia are composed of different cell populations that have distinct and even opposing functions. The two extremes of microglial polarization are termed classically activated M1 and alternatively activated M2 phenotypes.[9] Studies have revealed the two distinct functional polarization states of microglia in the spinal cord in nerve injury–induced neuropathic pain.[10–12] M1 microglia express CD16/32 and release pro-inflammatory factors, including inducible nitric oxide synthase (iNOS) and IL-1β, which were concomitant with the emergence of pathological pain.[13] Conversely, M2 microglia express CD206 and are associated with upregulation of anti-inflammatory mediators, such as arginase-1 (Arg-1), playing a vital role in reducing neuropathic pain.[14] Thus, shifting the polarization of microglia toward the M2 phenotype could potentially attenuate chronic neuropathic pain.[10,14,15] However, the status of microglial polarization in the spinal cord during the development of BCP remains unknown.

Dehydrocorydaline (DHC), an alkaloidal component isolated from *Rhizoma corydalis* (the dried tuber of *Corydalis yanhusuo W.T. Wang*), has been reported to ameliorate inflammatory pain with no toxicity by our previous studies.[16] In addition, it has been demonstrated to possess anti-inflammatory property and has been widely used to treat spastic pain, abdominal pain, and pain due to injury.[17,18] Moreover, previous studies have shown that DHC exerts anti-allergic and antitumor effects,[19,20] and that it could also suppress the elevated mitochondrial membrane potential in lipopolysaccharide-stimulated macrophage.[21] However, the effects of DHC on microglia have yet to be described, and it remains unknown whether DHC can attenuate BCP.

In this study, we used the mouse model of BCP to test the hypothesis that the imbalanced M1/M2 polarization of microglia toward the M1 phenotype contributes to the pro-inflammatory environment in the spinal cord and thus exacerbates the development of BCP. Furthermore, the study also investigated that DHC, one of the main constituents of *Rhizoma corydalis*, could attenuate BCP, with microglial polarization shifting toward the M2 phenotype in the spinal cord.

Materials and methods

Experimental animals

Adult male C3H/HeN mice (4–6 weeks old, weighing 20–25 g, obtained from Beijing Vital River Laboratory Animal Technology Co., Ltd. Beijing, China, SCXK JING 2012–0001) were used to for this study. The mice were housed in a temperature-controlled (21°C ± 1°C) room with a 12-h light/dark schedule, and allowed to get food and water ad libitum. All experimental procedures were performed under the approval of the Institutional Animal Care and Use Committee at the Affiliated Drum Tower Hospital of Medical Department of Nanjing University and in accordance with the ethical guidelines for the use of experimental animals.[22]

Cell culture and implantation

Osteosarcoma NCTC 2472 cells (American Type Culture Collection, Manassas, VA, USA, ATCC 2087787) were incubated in NCTC 135 medium (Sigma Aldrich, St. Louis, MO, USA) containing 10% equine serum (Gibco, Carlsbad, CA, USA) at 37°C in an atmosphere of 5% CO_2 and 95% air (Thermo Forma, OH, USA), and passaged twice per week according to the recommendations provided by the American Type Culture Collection.

The mouse model of BCP was established as previously described by Schwei et al.[23] Briefly, on day 0, after the mice were anesthetized with an intraperitoneal injection of pentobarbital sodium (50 mg/kg, 1% in normal saline (NS)), a right knee arthrotomy was performed. Subsequently, a 25-μl microsyringe was used to inject a volume of 20 μl α-minimal essential medium (α-MEM, Gibco, Carlsbad, CA) containing 2×10^5 NCTC 2472 cells (tumor group) or 20 μl α-MEM alone (Sham group) into the medullary cavity of the distal femur. The injection hole was then sealed using bone wax and irrigated with NS. Finally, the wound was sutured closed.

Drug preparation

DHC (VIC449, Vicmed biotech Co. Ltd., China), purity ≥ 98%, was dissolved in dimethyl sulfoxide (DMSO) and then diluted with NS prior to administration. On day 14 after osteosarcoma cell implantation, DHC was intraperitoneally administrated in tumor group mice at a dosage of 10 mg/kg, referred to our previous studies about inflammatory pain in mice[16] and based on our preliminary experiment. Meanwhile, a similar volume of 10% DMSO was also used for vehicle treatment in tumor group mice.

Pain behavior tests

All behavior tests were performed during the light phase by the experimenter who was blind to the treatment groups. The mice were allowed to acclimatize for at least 30 min before tests. The behavior tests were performed prior to operation (day 0) and then on days 4, 7, 10, 14, 21, and 28 after osteosarcoma cell implantation.

Besides, the mice were tested before (0 h) and at 1 h, 4 h, and 8 h after the administration of DHC and vehicles.

Paw withdrawal mechanical threshold (PWMT). PWMT was used to assess the mechanical allodynia using von Frey filaments (Stoelting, Wood Dale, IL, USA).[24] The mice were placed into individual transparent plexiglass compartments (10 cm × 10 cm × 15 cm) onto a metal mesh floor (graticule: 0.5 cm × 0.5 cm). Von Frey filaments (0.16, 0.4, 0.6, 1.0, 1.4, and 2.0 g) were applied to the right hind paw according to previous reports. The filaments were pressed vertically against the plantar surface with sufficient force to cause a slight bending against the paw and were held for 6–8 s. In addition, there was a 10-min interval between the two stimulations. Brisk withdrawal of the paw or paw flinching was regarded as a positive response, and each mouse was tested five times per stimulus strength. Finally, the lowest von Frey filament stimulus strength that produced three or more positive responses was regarded as the PWMT.

Number of spontaneous flinches (NSF). The mice were placed into individual plexiglass compartments (10 cm × 10 cm × 15 cm) and observed for 2 min to quantify the NSF of the right hind paw. Every lift that was not related to walking or grooming was considered one flinch. Each mouse was tested five times.

Immunofluorescence

The mice were deeply anesthetized with pentobarbital sodium (1% in NS, 50 mg/kg, i.p.) and perfused with NS via the ascending aorta, followed by 4% paraformaldehyde. Then the lumbar segments of the spinal cords were extracted quickly, postfixed in 4% paraformaldehyde, and dehydrated in 30% sucrose at 4°C. Serial frozen sections were cut in a freezing microtome into 20-μm thick slides, washed in PBS and blocked with 10% goat serum for 2 h at room temperature. Subsequently, the sections were incubated with primary antibodies overnight at 4°C. Then, they were incubated with secondary antibodies for 1.5 h at room temperature after washing in PBS. Finally, the sections were mounted on glass slides, air-dried, and covered with fluoroshield mounting medium with DAPI (Abcam, Cambridge, UK). Images were acquired using a Leica TCS SP8 multiphoton confocal microscope (Leica Microsystems, Wetzlar, Germany).

The following primary antibodies were used: rabbit anti-Iba-1 (1:500, Wako, Japan), rat anti-CD16/32 (1:100, BD biosciences, USA), mouse anti-CD206 (1:300, Abcam, Cambridge, UK), and rabbit anti-Arg-1 (1:100, Abcam, Cambridge, UK) antibodies. The secondary antibodies used in this study included the following: goat anti-rabbit (1:3000, Alexa 488-conjugated, ThermoFisher, Waltham, MA), goat anti-rat (1:2000, Alexa 594-conjugated, ThermoFisher), and goat anti-mouse (1:2000, Alexa 594-conjugated, ThermoFisher) antibodies.

Western blotting

After the mice were sacrificed under deep anesthesia with pentobarbital sodium (1% in NS, 50 mg/kg, i.p.), the lumbar spinal cord segments were quickly extracted and stored in liquid nitrogen. The collected tissue samples were weighed, homogenized in lysis buffer, and centrifuged. Then the supernatant was collected. Protein samples were separated on sodium dodecyl sulfate polyacrylamide gel electrophoresis and then transferred onto the polyvinylidene fluoride membranes (Millipore, Billerica, MA, USA). Subsequently, the membranes were blocked with 5% nonfat milk for 2 h at room temperature and incubated with the primary antibodies: rabbit anti-iNOS (1:500, Abcam, Cambridge, UK), rabbit anti-arginase I (1:600, Santa Cruz, CA), rabbit anti-IL-1β (1:700, Abcam, Cambridge, UK), and rabbit anti-IL-10 (1:500, Abcam, Cambridge, UK) at 4°C overnight. The membranes were then washed with TBST and incubated for 1.5 h at room temperature with peroxidase affinipure goat anti-rabbit secondary antibody (1:10000, Jackson ImmunoResearch Inc, West Grove, USA). Then, the membranes were visualized using a chemiluminescent HRP substrate (Millipore Corporation, MA, USA) in an automated chemiluminescence system (Tanon, Shanghai, China). β-actin was used as a loading control for total protein, and ImageJ software (NIH, Bethesda, MD, USA) was used to measure the gray value of each band.

Enzyme-linked immunosorbent assay

After the mice were sacrificed under deep anesthesia with pentobarbital sodium (1% in NS, 50 mg/kg, i.p.), the lumbar spinal cord segments were collected. The supernatants of tissue homogenates were collected and analyzed using enzyme-linked immunosorbent assay (ELISA) kits (Senbeijia, Nanjing, China) according to the manufacturer's instructions.

Statistical analysis

In behavioral assessments, two-way analysis of variance for repeated measures followed by post hoc tests (Bonferroni test) was used to analyze the differences between groups, and data are presented as the mean ± SD. Changes in immunofluorescence, western blotting results, and ELISA data were compared with the basal value using nonparametric Kruskal–Wallis test and Nemenyi test, and statistical comparisons between the groups were assessed with nonparametric Mann–

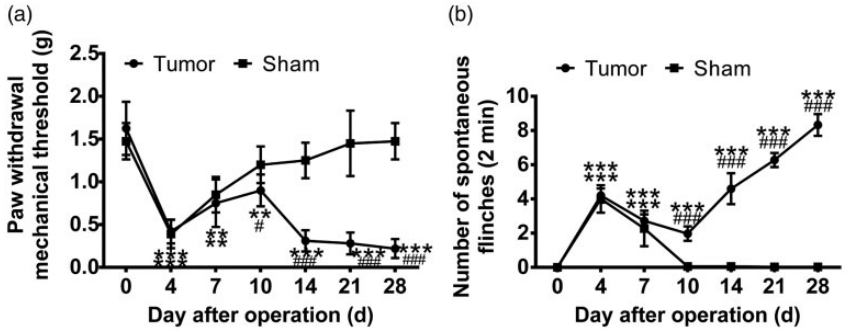

Figure 1. Changes in pain behaviors over time in tumor and sham group mice. (a) Paw withdraw mechanical threshold in response to von Frey filaments and (b) the number of spontaneous flinches that occurred during 2 min were tested on days 0, 4, 7, 10, 14, 21, and 28 after surgery in tumor and sham group mice. All data are presented as the mean ± SD. $^{*}p < 0.05$, $^{**}p < 0.01$, and $^{***}p < 0.001$ compared with day 0; $^{\#}p < 0.05$, $^{\#\#}p < 0.01$, and $^{\#\#\#}p < 0.001$ compared with the sham group mice; $n = 8$ mice per group.

Whitney test. Data are presented as the median with range. All statistical analyses were performed by IBM SPSS statistics version 21.0 (SPSS Inc., Chicago, IL, USA). Graph Pad Prism version 6 (GraphPad software, San Diego, CA, USA) was used to plot graphs, and a value of $p < 0.05$ was defined as statistically significant.

Results

BCP accelerates over time

Pain behaviors were tested to assess the pain development after osteosarcoma cell implantation. There was no significant difference in PWMT and NSF between tumor and sham groups prior to the operation. On day 4 after surgery, both tumor and sham group mice showed decreased PWMT of the right hind paw in response to von Frey filaments stimulation ($p < 0.001$, respectively), compared with basal value. The PWMT of the sham group mice had recovered to baseline since day 10. However, the PWMT of the tumor group mice did not return to the basic level and subsequently decreased from day 14 ($p < 0.001$) to day 28 ($p < 0.001$) (Figure 1(a)).

Both tumor and sham group mice displayed increased NSF on day 4 after surgery ($p < 0.001$, respectively), and the NSF of the sham group mice returned to the basic level on day 10. However, after decreasing from day 7 to day 10, the NSF of tumor group mice continuously increased from day 14 ($p < 0.001$) to day 28 ($p < 0.001$) (Figure 1(b)). These data suggest that BCP was established after osteosarcoma cell implantation and accelerated over time.

Polarization of microglia presents increased M1 and decreased M2 phenotypes during BCP development

To evaluate whether microglial polarization in the spinal cord participates in the development of BCP, molecular analyses of iNOS and Arg-1, which are preferentially induced in M1 and M2 microglia in the spinal cord, respectively, were next conducted. Western blotting results showed that the expression of iNOS increased on day 4 both in tumor and sham group mice ($p < 0.05$), compared with basal value, and there was no significant difference in the expression level of iNOS between tumor and sham group mice. Then, the expression of iNOS increased again on day 14 ($p < 0.05$) and kept at a high level until day 28 ($p < 0.01$) in tumor group mice. However, the level of iNOS recovered to baseline from day 7 in sham group mice (Figure 2(a) to (c)). Similarly, the expression of Arg-1 presented a transient increase on day 4 both in tumor and sham group mice ($p < 0.05$, respectively), and there was no significant difference in the expression level of Arg-1 between tumor and sham group mice, while it increased again and reached the peak on day 14 ($p < 0.01$) followed by a decline in tumor group mice (Figure 2(a), (b) and (d)).

Additionally, we further examined the expression of M1 (CD16/32/Iba-1) and M2 (CD206/Iba-1) phenotypes in the spinal cord, respectively, by immunofluorescence. As shown in the representative micrographs of immunostaining in the dorsal horn of ipsilateral spinal, Iba-1 was temporarily increased on day 4 ($p < 0.05$) and decreased to baseline from day 7, and then it gradually increased from day 14 ($p < 0.05$) to day 28 ($p < 0.01$) in the spinal cords of the tumor group mice. However, almost no Iba-1 expression was detected in the spinal cords of the sham group mice at late stages. Interestingly, most CD16/32 merged with Iba-1, and its expression exhibited changes similar to those observed for Iba-1, which indicated that M1 phenotype of microglia kept increasing from day 14 to day 28 after it displayed a transient increase on day 4 in tumor group mice (Figure 3(a) to (c)). For the expression of CD206, similarly, we found that in the spinal cords of the tumor group mice, after it was transiently increased on day 4

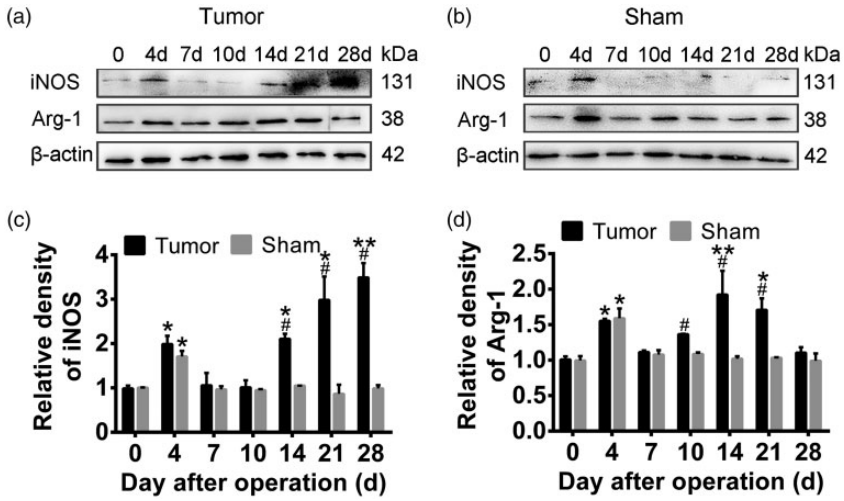

Figure 2. Changes of iNOS and Arg-1 expression during bone cancer pain development. (a and b) Representative blots of iNOS and Arg-1 in the spinal cords in tumor and sham group mice. (c and d) Quantification of iNOS and Arg-1 in the spinal cords in tumor and sham group mice on Western blotting. All data are presented as the median with range. $^{*}p < 0.05$, $^{**}p < 0.01$ compared with day 0; $^{\#}p < 0.05$, compared with the sham group mice; $n = 3$ mice per group.
iNOS: inducible nitric oxide synthase; Arg-1: arginase-1.

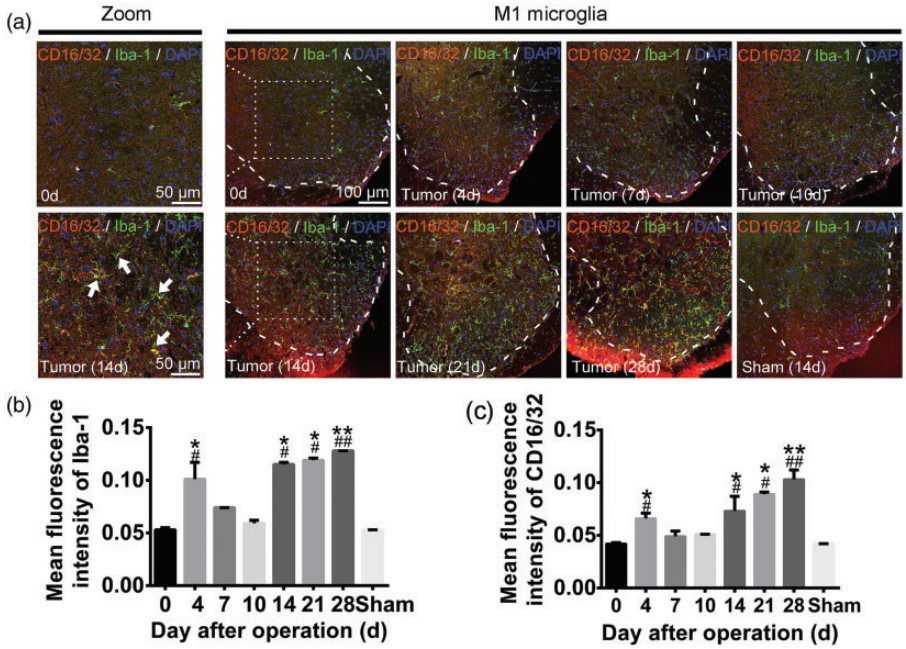

Figure 3. The alteration of M1 polarization of microglia during bone cancer pain development. (a) Double immunofluorescent staining of Iba-1 and CD16/32 in the spinal cords in tumor and sham (14 d) group mice. The enlarged images reveal that these two factors show colocalization. (b and c) Quantification of staining intensity of Iba-1 and CD16/32 in the spinal cords in tumor and sham (14 d) group mice. All data are presented as the median with range. $^{*}p < 0.05$, $^{**}p < 0.01$ compared with day 0; $^{\#}p < 0.05$, $^{\#\#}p < 0.01$ compared with the sham group mice; $n = 3$ mice per group.

($p < 0.05$), it peaked on day 14 ($p < 0.01$) and eventually decreased to baseline on day 28. No CD206 expression was detected in the spinal cords of the sham group mice at late stages. Furthermore, most CD206 expression showed colocalization with Iba-1 (Figure 4(a) and (c)). In addition, coimmunofluorescent staining also indicated that Arg-1 expression merged very well with that of CD206, and the change trend was consistent with that shown by western blotting (Figure 4(b) and (d)). These results indicated that M2 phenotype of microglia

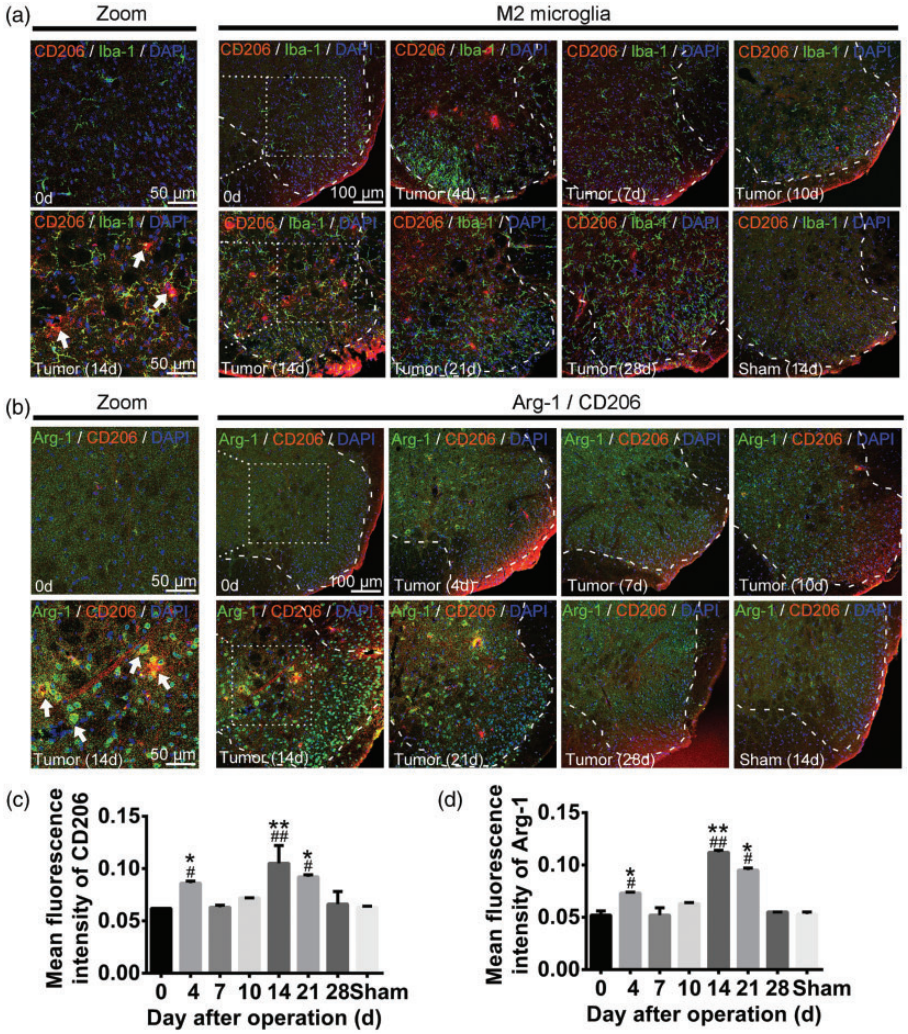

Figure 4. The alteration of M2 polarization of microglia and Arg-1 expression during bone cancer pain development. (a and c) Double immunofluorescent staining of CD206 and Iba-1 and quantification of CD206 in the spinal cords in tumor and sham (14 d) group mice. The enlarged images reveal that these two factors show colocalization. (b, d) Double immunofluorescent staining of Arg-1 and CD206 and quantification of Arg-1 in the spinal cords in tumor and sham (14 d) group mice. The enlarged images show that Arg-1 expression merged well with CD206 expression. All data are presented as the median with range. $^{*}p < 0.05$, $^{**}p < 0.01$ compared with day 0; $^{\#}p < 0.05$, $^{\#\#}p < 0.01$ compared with the sham group mice; $n = 3$ mice per group.
Arg-1: arginase-1.

transiently increased on day 4 after surgery, and then it reached the peak on day 14 followed by decreasing during the development of BCP.

Taken together, these findings revealed that the polarization of microglia in the spinal cord showed increased M1 and suppressed M2 phenotypes during the development of BCP.

IL-1β expression maintains increasing while IL-10 expression is suppressed during BCP development

To further investigate the alteration of inflammatory state accompanied by the imbalanced microglial polarization, we tested the expression of IL-1β and IL-10 in the spinal cord and blood in both tumor and sham groups of mice. As a classic proinflammatory factor, IL-1β can be released by M1 microglia. Compared with the basal value, the expression of IL-1β was temporarily higher from day 4 to day 7 after surgery in the spinal cords of both tumor ($p < 0.05$, respectively) and sham ($p < 0.05$, respectively) group mice, and then it decreased and recovered to baseline on day 10. But in tumor group mice, IL-1β expression elevated again on day 14 ($p < 0.05$) and maintained a high level until day 28 ($p < 0.05$) (Figure 5(a) to (c)). The results of ELISA also indicated similar alteration in IL-1β expression occurred in the spinal cord and blood (Figure 5(e) and (g)). IL-10, an anti-inflammatory mediator,

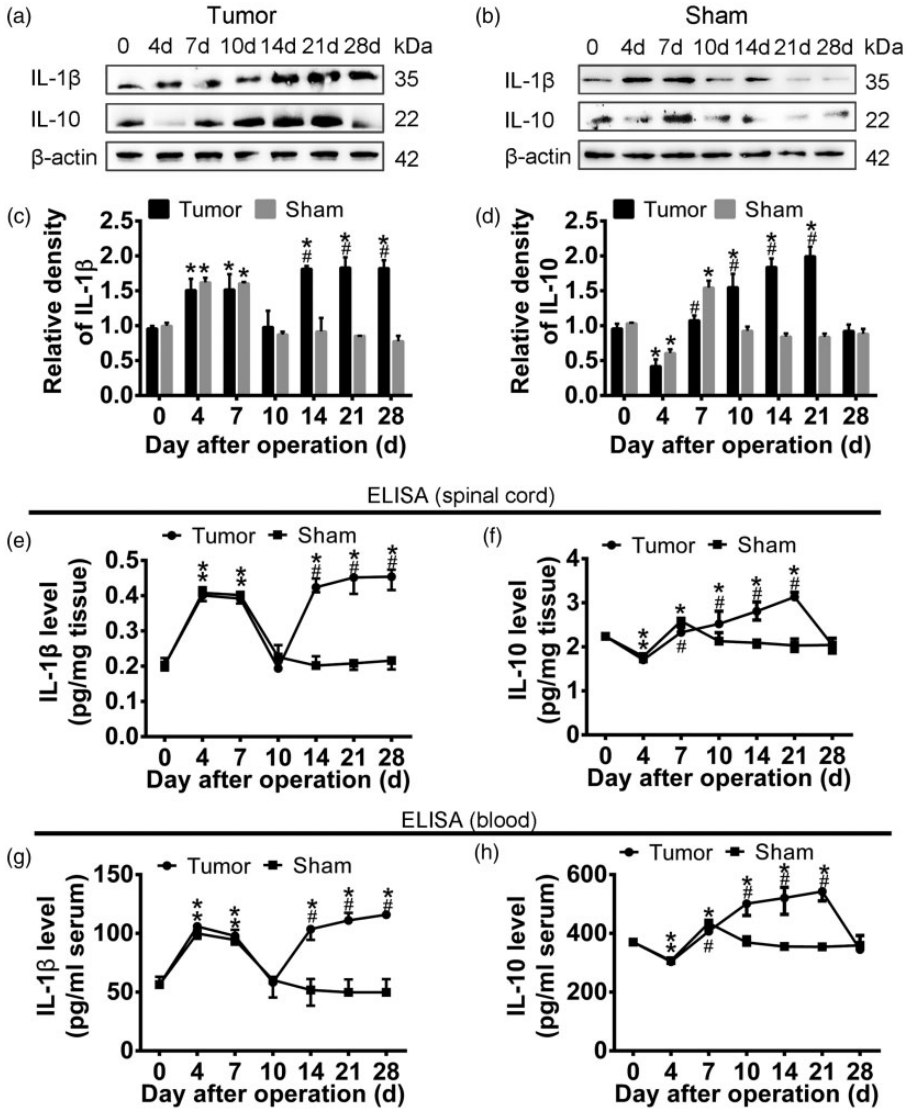

Figure 5. Changes of IL-1β and IL-10 expression during bone cancer pain development. (a and b) Representative blots of IL-1β and IL-10 in the spinal cords in tumor and sham group mice. (c and d) Quantification of IL-1β and IL-10 in the spinal cords in tumor and sham group mice on western blotting. (e and f) Results of ELISA showing the changes of IL-1β and IL-10 expression in the spinal cords in tumor and sham group mice. (g and h) Results of ELISA showing the changes of IL-1β and IL-10 expression in the blood in tumor and sham group mice. All data are presented as the median with range. $^{*}p < 0.05$ compared with day 0; $^{\#}p < 0.05$ compared with the sham group mice; n = 3 mice per group.

presented a transient reduction on day 4 after surgery both in tumor and sham group mice ($p < 0.05$, respectively), then it increased temporarily on day 7 ($p < 0.05$) and recovered to baseline afterwards in sham group mice. However, in spinal cords of tumor group mice, IL-10 increased from day 10 ($p < 0.05$) to day 21 ($p < 0.05$) and decreased to baseline on day 28 (Figure 5(a), (b), and (d)). Additionally, results of ELISA also indicated that the change of IL-10 in the blood was similar to that in the spinal cord (Figure 5 (f) and (h)). These data suggested that the pro-inflammatory response accelerated both in the spinal cord and blood with increased expression of IL-1β and inhibited expression of IL-10 during the development of BCP.

Intraperitoneal injection of DHC attenuates BCP

Based on the phenomena described above, we next examined whether DHC could attenuate BCP. DHC (10 mg/kg, i.p.) or vehicle was intraperitoneally injected to BCP mice on day 14 after surgery. PWMT and NSF were measured at various time points (preinjection (0 h), 1 h, 4 h, and 8 h after administration). Compared with

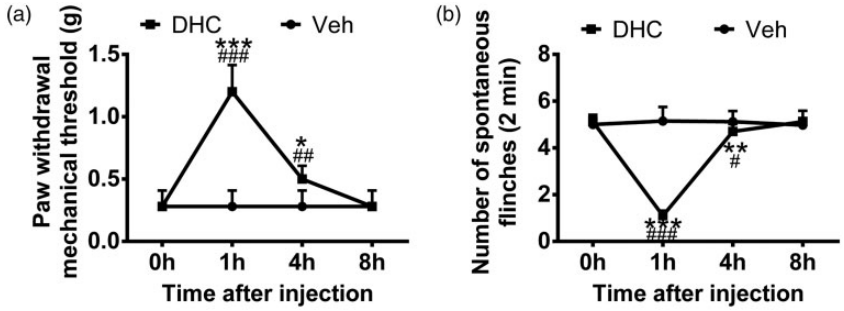

Figure 6. Intraperitoneal injection of DHC attenuates bone cancer pain. (a) Paw withdrawal mechanical threshold in response to von Frey filaments and (b) the number of spontaneous flinches during 2 min were tested before injection (0 h) and at 1 h, 4 h, and 8 h after DHC and vehicle administration. All data are presented as the mean ± SD. $^{*}p < 0.05$, $^{**}p < 0.01$, and $^{***}p < 0.001$ compared with pre-injected tumor group mice (0 h); $^{\#}p < 0.05$, $^{\#\#}p < 0.01$, and $^{\#\#\#}p < 0.001$ compared with the vehicle injected mice (Veh); n = 8 mice per group.
DHC, dehydrocorydaline.

preinjected and vehicle-injected mice, DHC injected mice showed significantly increased PWMT ($p < 0.001$, respectively) and decreased NSF ($p < 0.001$, respectively) at 1 h after injection. Then the PWMT gradually decreased and NSF gradually increased, and they completely returned to the preinjected level at 8 h (Figure 6). These data indicated that intraperitoneal injection of DHC significantly attenuated BCP.

Intraperitoneal injection of DHC shifts M1/M2 polarization of microglia toward the M2 phenotype

Next, we investigated the expression of M1 and M2 microglia after intraperitoneal injection of DHC to identify whether the analgesic effect of DHC was mediated by its influence on microglial polarization in the spinal cord. After intraperitoneal injection of DHC, the expression of iNOS was significantly downregulated at 1 h ($p < 0.05$, respectively) and 4 h ($p < 0.05$, respectively), compared with preinjected and vehicle-injected mice, while the level of Arg-1 was significantly upregulated at 1 h ($p < 0.05$, compared with preinjected mice; $p < 0.01$, compared with vehicle-injected mice) (Figure 7(a) to (c)). In immunofluorescent staining analysis, the expressions of Iba-1, CD16/32, CD206, and Arg-1 in the spinal cord were measured respectively (Figure 7(d)). The results showed no significant change of Iba-1 expression at all the time points (Figure 7(e)). Compared with preinjected and vehicle-injected mice, the expression of CD16/32 revealed a significant reduction at 1 h ($p < 0.05$, respectively) and 4 h ($p < 0.05$, respectively), and then it increased and reached the preinjected level at 8 h (Figure 7(f)). On the contrary, CD206 displayed a significant elevated expression at 1 h ($p < 0.05$, respectively) and returned to the preinjected level at 4 h (Figure 7(g)). Furthermore, the immunofluorescent staining analysis of Arg-1 showed a similar change with that of CD206 (Figure 7(h)).

These findings suggested that intraperitoneal injection of DHC inhibited the M1 microglia and shifted the polarization of microglia toward the M2 phenotype in the spinal cord.

Intraperitoneal injection of DHC suppresses the expression of IL-1β and increases the expression of IL-10

The inflammatory state in the spinal cord and blood was also changed after intraperitoneal injection of DHC. Compared with preinjected and vehicle-injected mice, the level of IL-1β in the spinal cord decreased significantly at 1 h ($p < 0.05$, respectively) and 4 h ($p < 0.05$, respectively), and then it recovered at 8 h after DHC administration. By contrast, a significant increase of IL-10 was observed at 1 h ($p < 0.01$, compared with preinjected mice; $p < 0.05$, compared with vehicle injected mice) and 4 h ($p < 0.05$, respectively) in the spinal cord, and then it decreased and reached the preinjected level at 8 h (Figure 8(a) to (c)). Similarly, results of ELISA also indicated the alterations of IL-1β and IL-10 levels in the blood, which were consisted with those in the spinal cord (Figure 8(d) and (e)). These results converged to suggest that DHC administration ameliorated the pro-inflammatory environment both in the spinal cords and blood of BCP mice.

Discussion

The present study provides evidence that activated microglia polarize and display increased M1 and decreased M2 phenotype in the spinal cord after osteosarcoma cell implantation, which contributes to the pro-inflammatory response and may accelerate the development of BCP. DHC administration, can attenuate BCP, inhibit the M1 phenotype, and increase M2 polarization, accompanied by suppressed expression of

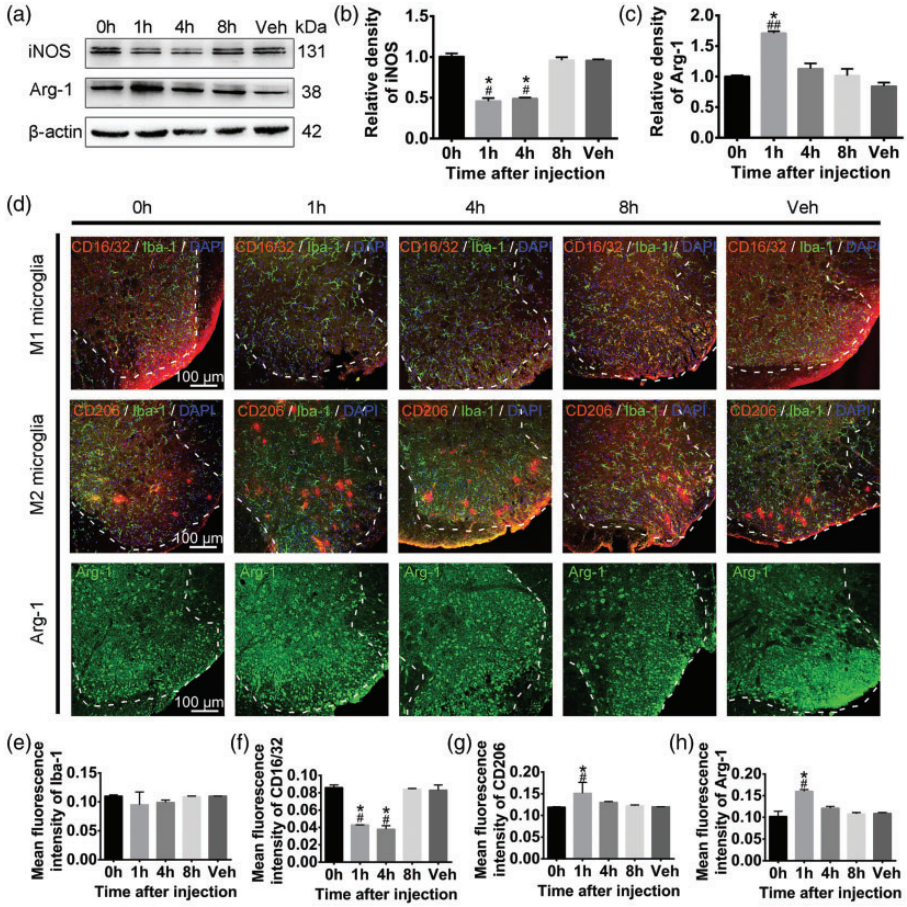

Figure 7. Intraperitoneal injection of DHC shifts M1/M2 polarization of microglia toward the M2 phenotype. (a-c) Representative blots and quantification of iNOS and Arg-1 expression in the spinal cords of pre-injected tumor group mice (0 h), DHC injected mice at 1 h, 4 h, and 8 h after injection, and vehicle injected mice (Veh). (d) Representative micrographs showing the changes of M1 phenotype, M2 phenotype, and Arg-1 expression in the spinal cords of pre-injected tumor group mice (0 h), DHC injected mice at 1 h, 4 h, and 8 h after injection, and vehicle injected mice (Veh). (e-h) Quantification of results showing the changes of Iba-1, CD16/32, CD206, and Arg-1 in the spinal cords of pre-injected tumor group mice (0 h), DHC injected mice at 1 h, 4 h, and 8 h after injection, and vehicle injected mice (Veh). All data are presented as the median with range. $^{*}p < 0.05$ compared with pre-injected tumor group mice (0 h); $^{\#}p < 0.05$, $^{\#\#}p < 0.01$ compared with the vehicle injected mice (Veh); n = 3 mice per group.
DHC, dehydrocorydaline; iNOS, inducible nitric oxide synthase; Arg-1, arginase-1.

IL-1β and elevated IL-10 level. These findings may help to provide a new explanation for the mechanisms of BCP development with an emphasis on imbalanced M1/M2 polarization in the spinal cord and indicate an avenue to treat BCP.

Studies have demonstrated that in mice with BCP, there are significant pathological changes in the lumbar segments of the spinal cord that receive input from nerve fibers that innervate the tumor-bearing tissue, and these changes further contribute to the generation and maintenance of cancer pain.[2,25] Microglia exert a function in the spinal cord similar to that of macrophages in the periphery and play an important role in promoting the development of BCP.[6,7,26–28] It is observed that microglia in resting state are highly dynamic in vivo. They continuously scan their immediate environment and interact with other elements in central nervous system (CNS). When the homeostasis of CNS is disrupted, microglia become rapidly activated by displaying morphological changes and upregulating microglial markers, playing an important role in central sensitization by releasing a plethora of neurotoxic substances.[4,5,29–31] Our present study further indicates that microglia in the spinal cord are significantly activated during the development of BCP, as evidenced by the increased expression of Iba-1 in the spinal cord from day 14 to day 28 after osteosarcoma cell implantation.

An increasing number of studies now consider that microglia are highly plastic cells that can assume diverse phenotypes and engage in different functional programs in response to specific changes in CNS. Similar to the classical M1 versus the alternative M2 paradigm defined

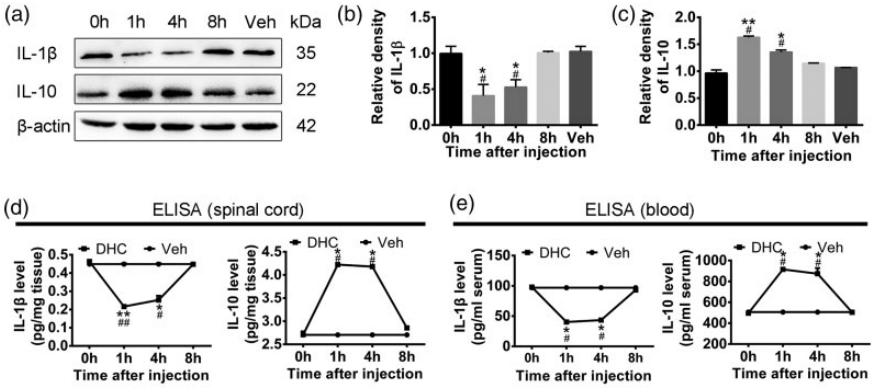

Figure 8. Intraperitoneal injection of DHC suppresses the expression of IL-1β and elevates the expression of IL-10. (a-c) Representative blots and quantification of IL-1β and IL-10 expression in the spinal cords of pre-injected tumor group mice (0 h), DHC injected mice at 1 h, 4 h, and 8 h after injection, and vehicle injected mice (Veh). (d, e) Results of ELISA showing the expression of IL-1β and IL-10 in the spinal cords and blood of pre-injected tumor group mice (0 h), DHC and vehicle injected mice at 1 h, 4 h, and 8 h after injection. All data are presented as the median with range. $^{*}p < 0.05$, $^{**}p < 0.01$ compared with the pre-injected tumor group mice (0 h); $^{\#}p < 0.05$, $^{\#\#}p < 0.01$ compared with the vehicle injected mice (Veh); n = 3 mice per group.
DHC, dehydrocorydaline.

for macrophages, M1 and M2 polarization of microglia has also been recently coined and characterized in various CNS disorders like stroke,[32,33] traumatic brain injury,[34] and spinal cord injury.[10,12] Classically activated M1 microglia typically release destructive pro-inflammatory mediators that contribute to the tissue damage. iNOS is one of the most interesting M1 microglial polarization markers, and it has been implicated in the pathology of spinal cord injury and neuropathic pain.[35–37] IL-1β can be produced by M1 microglia, and intrathecal administration of this cytokine has been demonstrated to have algesic properties.[38,39] On the contrary, alternatively activated M2 phenotype produces numerous protective and trophic factors and underlies the protective effects.[9,15,40,41] The M1/M2 polarization plays a pivotal role in controlling the balance between promotion and suppression of inflammation. Moreover, adoptive transfer of M2 macrophages has been reported to reduce neuropathic pain.[42] Modulating the factors in the microenvironment to reduce excessive M1 polarization and enhance M2 polarization may be a way for tissue repair [41,43–47] and could be a strategy for treatment of neuropathic pain.[10,14,48] However, there is no report about whether M1/M2 polarization participates in the development of BCP currently. An improved understanding of phenotype dynamics of M1 and M2 microglia in the spinal cord is likely to advance our knowledge of BCP and to be critical for BCP treatment in the future.

In the current study, we observed an imbalanced microglial polarization of M1 and M2 in the spinal cord in the mouse model of BCP. On day 4 after surgery, microglia in the spinal cord were activated and presented increased M1 and M2 phenotypes with acute pain after surgery, as evidenced by the increased expression of CD16/32 and CD206 in Iba-1^{+} cells. Soon after the BCP was established, the microglia were significantly activated and assumed both M1 and M2 phenotypes in the spinal cords on day 14. Subsequently, the M1 microglia continuously increased from day 14 to day 28 with the development of BCP. However, after the M2 polarization showed a transient increase on day 14, it was downregulated and completely phased out on day 28. The present study further suggests that M1 microglia are "sick" cells as they increased production of pro-inflammatory factors, including iNOS and IL-1β, which were elevated from day 14 to day 28 in the spinal cords of tumor group mice. In contrast, M2 microglia are "healthy" cells with elevated secretion of ant-inflammatory mediators with antinociceptive properties, like Arg-1. The anti-inflammatory cytokine IL-10, which could be partially produced by M2 microglia,[49] was also inhibited on day 28. Furthermore, IL-10 has been demonstrated to reduce the inflammatory pain[50] and induce M2 polarization.[51] It is possible that the failed M2 microglia response may contribute to the change from protective responses to harmful results because of failed inflammation control. Such M1 shift has also been reported in models of neuropathic pain, suggesting that the microglia phenotypic change may be a common pathological mechanism underlying pain development.[10,14,48] It is thus possibly conceivable that the imbalanced polarization of microglia toward the M1 phenotype expands the inflammatory response in the spinal cord at late stages and leads to the development of BCP.

Rhizoma corydalis has been used to treat spastic pain, abdominal pain, and pain due to injury for thousands

of years in the traditional Chinese medical system. DHC, an alkaloid compound isolated from Rhizoma corydalis, has been reported to exert anti-allergic and anti-tumor effects.[19,20] In addition, our recent studies have reported that DHC has antinociceptive effect on inflammatory pain with no toxicity.[16] In the present study, we investigated the effects of DHC on BCP and microglial polarization in the spinal cord. Our results showed that BCP was significantly ameliorated at 1 h after DHC was intraperitoneally injected at a dosage according to the previous studies. Microglial polarization in the spinal cord presented suppressed M1 phenotype and increased M2 phenotype, while the expression of Iba-1 showed no obvious alteration. As a representative mediator of M1 microglia, iNOS was also downregulated after DHC administration. Meanwhile, the expression of Arg-1, which was produced by M2 microglia, increased at 1 h, and these changes were consistent with the behavioral alterations following DHC treatment. Additionally, IL-1β presented a significantly lower level and the expression of IL-10 increased both in the spinal cord and blood after DHC injection, which indicated that DHC reduced the systemic inflammatory response of BCP mice. Thus, it is possible that intraperitoneal administration of DHC shifted the microglia polarization toward the M2 phenotype and modulated inflammatory environment in the body, especially in the spinal cord. Moreover, we noted that DHC administration did not cause any aberrant behaviors or abnormalities in the activity, diet, hair, feces or body weight in the mice, which indicated that DHC did not cause any acute or chronic toxicity. These results suggest that BCP therapies should be shifted from simply suppressing microglial activation toward adjusting the imbalance between beneficial and detrimental microglial responses. Drugs with the ability to block the shift toward M1 and promote the M2 polarization could be beneficial for BCP treatment.

Many questions still remain about M1 and M2 polarization and the phenotypic shift during the development of BCP. For example, as there was no specific inhibitor or agonist for M1 and M2 microglia, we could not modulate the M1 or M2 phenotypes directly to demonstrate their role in BCP. Thus, we used DHC, which has been observed to have antinociceptive properties by our previous studies in the acetic acid-induced writing tests and the formalin paw tests in mice,[16] to further test whether BCP can be attenuated and whether it involves changes in microglial polarization. Additionally, the exogenous signals that induce the microglia phenotype shift have not yet been identified. Several studies consider that tissue microenvironment influences the terminal differentiation of microglia, suppressing an M2 phenotype while inducing the M1 polarization in response to sequential stimuli.[33,42,52,53] The systemic inflammatory response may affect the microenvironment in the spinal cord, which could in turn regulate the microglial polarization, possibly. Moreover, it is possible that M2-type microglia can convert to the M1 phenotype and exert the toxic effects in spinal cord, but it remains to identify the molecular switches that control such a dramatic phenotypic change. Additionally, our study tested the alteration of cytokines in the blood and spinal cord, including IL-1β and IL-10, to evaluate the inflammatory environment. The level of IL-1β and IL-10 in the spinal cord could also indicate the alteration of microglial polarization. However, the alteration of IL-1β and IL-10 expression is related but not totally ascribed to the M1/M2 polarization of microglia, as other cells like astrocyte in the spinal cord can also produce IL-1β.[54] It also needs to be confirmed by analyzing other cell types in the spinal cord in further researches.

In conclusion, the present study indicates for the first time that the development of BCP is associated with the imbalanced polarization of microglia toward M1 in the spinal cord. Notably, DHC administration attenuated BCP, inhibited the M1 phenotype, and shifted the microglial polarization toward M2 in the spinal cord, which was accompanied by suppressed inflammatory response both in the spinal cord and blood. These findings suggest the role of M1/M2 polarization of microglia in BCP development, and provide evidence for the potential pharmaceutical application of DHC in BCP therapies.

Author Contributions

Wenwen Huo and Zhengliang Ma conceived and designed the research. Wenwen Huo performed immunofluorescence and edited the manuscript. Ying Zhang prepared the animals and cells to establish bone cancer pain models. Yue Liu performed the cell implantations. Yishan Lei contributed to the intraperitoneal injection and performed western blotting. Yulin Huang and Rao Sun contributed to revising the manuscript. Wei Zhang analyzed the data. Yanting Mao performed pain behavioral assessments. Chenchen Wang performed enzyme-linked immunosorbent assays. Zhengliang Ma and Xiaoping Gu coordinated and directed the project. All authors read and approved the final manuscript.

Declaration of Conflicting Interests

The author(s) declared no potential conflicts of interest with respect to the research, authorship, and/or publication of this article.

Funding

The author(s) disclosed receipt of the following financial support for the research, authorship, and/or publication of this article: This study was supported by the National Natural Science Foundation of China (Nos. 81671087, 81471129, 81371207, and 81771142) and a grant from the Department

of Health of Jiangsu Province of China (Jiangsu Provincial Key Medical Discipline).

References

1. van den Beuken-van Everdingen MH, de Rijke JM, Kessels AG, Schouten HC, van Kleef M and Patijn J. Prevalence of pain in patients with cancer: a systematic review of the past 40 years. *Ann Oncol* 2007; 18: 1437–1449.
2. Mantyh P. Bone cancer pain: causes, consequences, and therapeutic opportunities. *Pain* 2013; 154: S54–S62.
3. Falk S and Dickenson AH. Pain and nociception: mechanisms of cancer-induced bone pain. *JCO*. 2014; 32: 1647–1654.
4. Nimmerjahn A, Kirchhoff F and Helmchen F. Resting microglial cells are highly dynamic surveillants of brain parenchyma in vivo. *Science* 2005; 308: 1314–1318.
5. Ji RR, Berta T and Nedergaard M. Glia and pain: is chronic pain a gliopathy? *Pain* 2013; 154: S10–S28.
6. Liu M, Yao M, Wang H, Xu L, Zheng Y, Huang B, Ni H, Xu S, Zhou X and Lian Q. P2Y12 receptor-mediated activation of spinal microglia and p38MAPK pathway contribute to cancer-induced bone pain. *J Pain Res* 2017; 10: 417–426.
7. Hu XF, He XT, Zhou KX, Zhang C, Zhao WJ, Zhang T, Li JL, Deng JP and Dong YL. The analgesic effects of triptolide in the bone cancer pain rats via inhibiting the upregulation of HDACs in spinal glial cells. *J Neuroinflammation* 2017; 14: 213.
8. Mao-Ying QL, Wang XW, Yang CJ, Li X, Mi WL, Wu GC and Wang YQ. Robust spinal neuroinflammation mediates mechanical allodynia in Walker 256 induced bone cancer rats. *Mol Brain* . 2012; 5: 16.
9. Hu X, Leak RK, Shi Y, Suenaga J, Gao Y, Zheng P and Chen J. Microglial and macrophage polarization—new prospects for brain repair. *Nat Rev Neurol* 2015; 11: 56–64.
10. Li Z, Wei H, Piirainen S, Chen Z, Kalso E, Pertovaara A and Tian L. Spinal versus brain microglial and macrophage activation traits determine the differential neuroinflammatory responses and analgesic effect of minocycline in chronic neuropathic pain. *Brain, Behavior, and Immunity* 2016; 58: 107–117.
11. Kobiela K A, Byrnes KR, Grunberg NE, Kasper CE, Osborne L, Pryor B, Tosini NL, Wu X and Anders JJ. Characterization of macrophage/microglial activation and effect of photobiomodulation in the spared nerve injury model of neuropathic pain. *Pain Med* 2017; 18: 932–946.
12. Xu F, Huang J, He Z, Chen J, Tang X, Song Z, Guo Q and Huang C. Microglial polarization dynamics in dorsal spinal cord in the early stages following chronic sciatic nerve damage. *Neurosci Lett* 2016; 617: 6–13.
13. Kuner R. Spinal excitatory mechanisms of pathological pain. *Pain* 2015; 156 Suppl 1: 1: S11–S17.
14. Gong X, Chen Y, Fu B, Jiang J and Zhang M. Infant nerve injury induces delayed microglial polarization to the M1 phenotype, and exercise reduces delayed neuropathic pain by modulating microglial activity. *Neuroscience* 2017; 349: 76–86.
15. Kigerl KA, Gensel JC, Ankeny DP, Alexander JK, Donnelly DJ and Popovich PG. Identification of two distinct macrophage subsets with divergent effects causing either neurotoxicity or regeneration in the injured mouse spinal cord. *J Neurosci* 2009; 29: 13435–13444.
16. Yin ZY, Li L, Chu SS, Sun Q, Ma ZL and Gu XP. Antinociceptive effects of dehydrocorydaline in mouse models of inflammatory pain involve the opioid receptor and inflammatory cytokines. *Sci Rep* 2016; 6: 27129.
17. Wang C, Wang S, Fan G and Zou H. Screening of antinociceptive components in Corydalis yanhusuo W.T. Wang by comprehensive two-dimensional liquid chromatography/tandem mass spectrometry. *Anal Bioanal Chem* 2010; 396: 1731–1740.
18. Kubo M, Matsuda H, Tokuoka K, Ma S and Shiomoto H. Anti-inflammatory activities of methanolic extract and alkaloidal components from Corydalis tuber. *Biol Pharm Bull* 1994; 17: 262–265.
19. Matsuda H, Tokuoka K, Wu J, Shiomoto H and Kubo M. Inhibitory effects of dehydrocorydaline isolated from Corydalis tuber against type I-IV allergic models. *Biol Pharm Bull* 1997; 20: 431–434.
20. Xu Z, Chen X, Fu S, Bao J, Dang Y, Huang M, Chen L and Wang Y. Dehydrocorydaline inhibits breast cancer cells proliferation by inducing apoptosis in MCF-7 cells. *Am J Chin Med* 2012; 40: 177–185.
21. Ishiguro K, Ando T, Maeda O, Watanabe O and Goto H. Dehydrocorydaline inhibits elevated mitochondrial membrane potential in lipopolysaccharide-stimulated macrophages. *Int Immunopharmacol* 2011; 11: 1362–1367.
22. Zimmermann M. Ethical guidelines for investigations of experimental pain in conscious animals. *Pain* 1983; 16: 109–110.
23. Schwei MJ, Honore P, Rogers SD, Salak-Johnson JL, Finke MP, Ramnaraine ML, Clohisy DR and Mantyh PW. Neurochemical and cellular reorganization of the spinal cord in a murine model of bone cancer pain. *J Neurosci* 1999; 19: 10886–10897.
24. Chaplan SR, Bach FW, Pogrel JW, Chung JM and Yaksh TL. Quantitative assessment of tactile allodynia in the rat paw. *J Neurosci Meth* 1994; 53: 55–63.
25. Mantyh PW. Bone cancer pain: from mechanism to therapy. *Curr Opin Palliat Care* 2014; 8: 83–90.
26. Zhang MY, Liu YP, Zhang LY, Yue DM, Qi DY, Liu GJ and Liu S. Levo-tetrahydropalmatine attenuates bone cancer pain by inhibiting microglial cells activation. *Mediat Inflamm* 2015; 2015: 1.
27. Hu XM, Liu YN, Zhang HL, Cao SB, Zhang T, Chen LP and Shen W. CXCL12/CXCR4 chemokine signaling in spinal glia induces pain hypersensitivity through MAPKs-mediated neuroinflammation in bone cancer rats. *J Neurochem* 2015; 132: 452–463.
28. Bu H, Shu B, Gao F, Liu C, Guan X, Ke C, Cao F, Hinton AO, Jr., Xiang H, Yang H, Tian X and Tian Y. Spinal IFN-gamma-induced protein-10 (CXCL10) mediates metastatic breast cancer-induced bone pain by activation of microglia in rat models. *Breast Canc Res Treat* 2014; 143: 255–263.

29. Shemer A and Jung S. Differential roles of resident microglia and infiltrating monocytes in murine CNS autoimmunity. *Semin Immunopathol* 2015; 37: 613–623.
30. Peng J, Gu N, Zhou L, B Eyo U, Murugan M, Gan W-B and Wu L-J. Microglia and monocytes synergistically promote the transition from acute to chronic pain after nerve injury. *Nat Comms* 2016; 7: 12029.
31. Echeverry S, Shi XQ and Zhang J. Characterization of cell proliferation in rat spinal cord following peripheral nerve injury and the relationship with neuropathic pain. *Pain* 2008; 135: 37–47.
32. Hu X, Li P, Guo Y, Wang H, Leak RK, Chen S, Gao Y and Chen J. Microglia/macrophage polarization dynamics reveal novel mechanism of injury expansion after focal cerebral ischemia. *Stroke* 2012; 43: 3063–3070.
33. Cheon SY, Kim EJ, Kim JM, Kam EH, Ko BW and Koo BN. Regulation of microglia and macrophage polarization via apoptosis signal-regulating kinase 1 silencing after ischemic/hypoxic injury. *Front Mol Neurosci* 2017; 10: 261.
34. Wang G, Zhang J, Hu X, Zhang L, Mao L, Jiang X, Liou AK, Leak RK, Gao Y and Chen J. Microglia/macrophage polarization dynamics in white matter after traumatic brain injury. *J Cereb Blood Flow Metab*. 2013; 33: 1864–1874.
35. Makuch W, Mika J, Rojewska E, Zychowska M and Przewlocka B. Effects of selective and non-selective inhibitors of nitric oxide synthase on morphine- and endomorphin-1-induced analgesia in acute and neuropathic pain in rats. *Neuropharmacology* 2013; 75: 445–457.
36. Pearse DD, Chatzipanteli K, Marcillo AE, Bunge MB and Dietrich WD. Comparison of iNOS inhibition by antisense and pharmacological inhibitors after spinal cord injury. *J Neuropathol Exp Neurol* 2003; 62: 1096–1107.
37. Chatzipanteli K, Garcia R, Marcillo AE, Loor KE, Kraydieh S and Dietrich WD. Temporal and segmental distribution of constitutive and inducible nitric oxide synthases after traumatic spinal cord injury: effect of aminoguanidine treatment. *J Neurotrauma* 2002; 19: 639–651.
38. Mika J, Korostynski M, Kaminska D, Wawrzczak-Bargiela A, Osikowicz M, Makuch W, Przewlocki R and Przewlocka B. Interleukin-1 alpha has antiallodynic and antihyperalgesic activities in a rat neuropathic pain model. *Pain* 2008; 138: 587–597.
39. Kawasaki Y, Zhang L, Cheng JK and Ji RR. Cytokine mechanisms of central sensitization: distinct and overlapping role of interleukin-1beta, interleukin-6, and tumor necrosis factor-alpha in regulating synaptic and neuronal activity in the superficial spinal cord. *J Neurosci* 2008; 28: 5189–5194.
40. Franco R and Fernández-Suárez D. Alternatively activated microglia and macrophages in the central nervous system. *Progress in Neurobiology* 2015; 131: 65–86.
41. Prinz M and Priller J. Microglia and brain macrophages in the molecular age: from origin to neuropsychiatric disease. *Nat Rev Neurosci* . 2014; 15: 300–312.
42. Pannell M, Labuz D, Celik MO, Keye J, Batra A, Siegmund B and Machelska H. Adoptive transfer of M2 macrophages reduces neuropathic pain via opioid peptides. *J Neuroinflammation*. 2016; 13: 262.
43. David S, Kroner A. Repertoire of microglial and macrophage responses after spinal cord injury. *Nat Rev Neurosci*. 2011; 12: 388–399.
44. Martinez FO, Helming L and Gordon S. Alternative activation of macrophages: an immunologic functional perspective. *Annu Rev Immunol* 2009; 27: 451–483.
45. Liu C, Li Y, Yu J, Feng L, Hou S, Liu Y, Guo M, Xie Y, Meng J, Zhang H, Xiao B and Ma C. Targeting the shift from M1 to M2 macrophages in experimental autoimmune encephalomyelitis mice treated with fasudil. *PloS One* 2013; 8: e54841–e54802. 2013//19.
46. Mikita J, Dubourdieu-Cassagno N, Deloire MS, Vekris A, Biran M, Raffard G, Brochet B, Canron MH, Franconi JM, Boiziau C and Petry KG. Altered M1/M2 activation patterns of monocytes in severe relapsing experimental rat model of multiple sclerosis. Amelioration of clinical status by M2 activated monocyte administration. *Mult Scler* 2011; 17: 2–15.
47. Mills CD and Ley K. M1 and M2 macrophages: the chicken and the egg of immunity. *J Innate Immun* 2014; 6: 716–726.
48. Xu N, Tang XH, Pan W, Xie ZM, Zhang GF, Ji MH, Yang JJ, Zhou MT and Zhou ZQ. Spared nerve injury increases the expression of microglia m1 markers in the prefrontal cortex of rats and provokes depression-like behaviors. *Front Neurosci*. 2017; 11: 209.
49. Nakagawa Y and Chiba K. Diversity and plasticity of microglial cells in psychiatric and neurological disorders. *Pharmacol Therapeut* 2015; 154: 21–35.
50. Zhou Z, Peng X, Hao S, Fink DJ and Mata M. HSV-mediated transfer of interleukin-10 reduces inflammatory pain through modulation of membrane tumor necrosis factor alpha in spinal cord microglia. *Gene Ther* 2008; 15: 183–190.
51. Mantovani A, Sozzani S, Locati M, Allavena P and Sica A. Macrophage polarization: tumor-associated macrophages as a paradigm for polarized M2 mononuclear phagocytes. *Trends Immunol* 2002; 23: 549–555. 2002/10/29.
52. Stout RD, Jiang C, Matta B, Tietzel I, Watkins SK and Suttles J. Macrophages sequentially change their functional phenotype in response to changes in microenvironmental influences. *J Immunol* 2005; 175: 342–349.
53. Mosser DM and Edwards JP. Exploring the full spectrum of macrophage activation. *Nat Rev Immunol* 2008; 8: 958–969.
54. Piotrowska A, Kwiatkowski K, Rojewska E, Makuch W and Mika J. Maraviroc reduces neuropathic pain through polarization of microglia and astroglia—evidence from in vivo and in vitro studies. *Neuropharmacology* 2016; 108: 207–219.